energies

MDPI

Article

A Corrected Equilibrium Manifold Expansion Model for Gas Turbine System Simulation and Control

Linhai Zhu, Jinfu Liu *, Yujia Ma, Weixing Zhou and Daren Yu

School of Energy Science and Engineering, Harbin Institute of Technology, Harbin 150001, China; zhulinhaihit@outlook.com (L.Z.); mayujiahit@outlook.com (Y.M.); zhouweixing@hit.edu.cn (W.Z.); yudaren@hit.edu.cn (D.Y.)

* Correspondence: jinfuliu@hit.edu.cn; Tel.: +86-189-4603-2945

Received: 21 August 2020; Accepted: 16 September 2020; Published: 18 September 2020

Abstract: During recent decades, the equilibrium manifold expansion (EME) model has been considered as a powerful identification tool for complex industrial systems with the aim of system control and simulation. Based on a two-step "dynamic and static" identification method, an approximate nonlinear state-space model is built by using multiple polynomials. However, the existing identification method is only suitable for single-input (SI) systems, but not for multi-input (MI) systems, where EME models cannot guarantee global calculation stability. For solving such a problem, this paper proposes a corrected equilibrium manifold expansion (CEME) model based on gas turbine prior knowledge. The equilibrium manifold is extended in dimension by introducing similarity equations instead of the high dimensional polynomial fitting. The dynamic similarity criterion of similarity theory guarantees the global stability of the CEME model. Finally, the comparative test between the CEME model and the existing MI-EME model is carried out through case studies involving data that are generated by a general turbofan engine simulation. Simulations show superior precision and calculation stability of the proposed model in capturing nonlinear behaviors of the gas turbine engine.

Keywords: gas turbine; system identification; corrected equilibrium manifold expansion model; multiple input multiple output; similarity theory

1. Introduction

Gas turbine (GT) engines provide power for airplanes, ships, and industrial equipment, and reliable and efficient operation is crucial to their safety and performance. Unexpected faults and improper control lead to unplanned maintenance of equipment [1]. Since the cost of unplanned service interruption is usually significantly higher than the cost of performing preventative maintenance and returning [2], sensitive fault detection, and isolation systems and robust control systems are essential, in both of which an accurate model describing engine behaviors is very important [3].

The demand for enhanced and reliable performance of models is ever increasing while an urgent demand for shorting design cycles, minimizing inspection and reducing costs is required. With significant interest to expand the performance of models, there is also the need for designing smaller and more flexible nonlinear models. Therefore, the need to use simple and nonlinear structural models is increasing in engineering applications.

Equilibrium manifold expansion (EME) model has gained more and more attention because of its simplicity and clear structure. The EME model is an approximate nonlinear model developed from the Jacobian Linearization model [4], which has been widely used in the field of system simulation [5,6], system control [7,8], and fault diagnosis [9]. It is generally known that the Jacobian linearization model is only valid near its equilibrium point, but the EME model is a global nonlinear model, which can deal

with the entire range of operation conditions [10]. Based on the implicit function rule and a two-step "dynamic and static" identification method, it is easy to build an EME model by using a small amount of data. Moreover, the EME model has a clear analytical form and a simple model structure to ensure simulation requirements and real-time computing. Thus far, the research on the EME model mainly focuses on the theoretical research [4], identification method [11], the role of scheduling variables [7], and engineering application [12,13]. However, all of the above studies center on single input (SI) EME models. Although an EME model can be theoretically extended to a multiple-input (MI) model, due to the shortcomings of the identification of equilibrium manifold (EM) fitting, it is difficult to build an MI-EME model with the global computational stability for GTs. Firstly, enough equilibrium points are needed to obtain a large enough range of EM. Additionally, the EM dimension increases with the increase of the input variable dimension. This means that the number of steady-state points will increase exponentially. However, in the actual operation of an aero-engine, it is not easy to find enough steady-state points to meet the needs of modeling. Secondly, the condition of the least square identification of dynamic parameters with constraints is that the input variables must step at the same time, which results in the MI-EME model only capturing nonlinear behaviors of the aero-engine in the given trajectory, and cannot ensure the global computational stability of the model. Furthermore, the condition of the synchronous step is too strict to be realized in practice. For example, it is not easy to realize the step change of engine inlet conditions (including engine inlet total temperature and engine inlet total pressure, called EIC for short) no matter whether in the actual operation of the engine or the ground test.

For solving the above problems, this paper proposes a corrected equilibrium manifold expansion (CEME) model by integrating the prior knowledge of gas turbines into the existing identification method. The CEME model is an MI-EME model with three inputs including fuel flow, engine inlet total temperature, and engine inlet total pressure (the latter two can be collectively referred to as engine inlet conditions, namely, EIC). Based on the similarity theory, a one-dimensional EM with similarity equations is transformed into a corrected equilibrium manifold (CEM) that is equivalent to a high-dimensional EM. Benefitting from such a transformation, the requirements of modeling data are reduced while the introduction of nonlinear equations reduces the fitting error caused by the polynomial fitting. Further, the CEME model can ensure the global stability of calculation by adjusting the dynamic matrixes and CEM in real-time. For verifying the effectiveness of the proposed method, some studies are conducted for a general aircraft engine prototype. Simulations show superior precision and computational stability of the proposed model in capturing nonlinear behaviors of a turbofan engine than the MI-EME model identified by the existing identification method.

The rest of this paper is organized as follows: Section 2 presents the EME model as well as its benefits and drawbacks in detail. In Section 3, the conception of the CEME model is proposed. Section 4 presents the CEME modeling experiment and simulation analysis. In Section 5, the comparative experiment indicates the superior performance of the proposed methodology with regards to calculation stability and estimation accuracy. Finally, Section 6 provides some concluding remarks.

2. EME Model Description and Discussions

2.1. EME Model Structure

In general, a nonlinear system can be simply described as follows:

$$\begin{cases} \dot{X} = f(X, U) \\ Y = g(X, U) \end{cases} \tag{1}$$

where X is the state vector, U is the input vector, Y is the output vector, $X \in R^n, U \in R^m, Y \in R^k$. f and g are smooth nonlinear functions.

In general, there are many equilibrium points for the nonlinear dynamical system (1). All equilibrium points of the nonlinear system constitute the equilibrium family:

$$\{(X_e, U_e, Y_e) \big| f(X_e, U_e) = 0, Y_e = g(X_e, U_e)\} \tag{2}$$

where the subscript '*e*' means the equilibrium point.

According to the theorem of implicit function [14], there must be a continuous mapping relationship between steady states of state variables of the nonlinear system (1). Additionally, equilibrium points of the nonlinear system (1) are generally continuous under the concept of the manifold [15]. Thus, the set of such equilibrium points can be considered as the equilibrium family of the nonlinear system (1). If there are n equations with $n + m$ variables for the steady state equations of the equilibrium family (2), $n + m$ variables can be represented by arbitrary m variables. In other words, an m-dimension vector α, called the scheduling variable in this paper, can represent the whole equilibrium family (2) as shown below. After the mapping relation is found, EM can be established and parameterized by the scheduling variable α.

$$\begin{cases} X_e = X_e(\alpha) \\ U_e = U_e(\alpha) \\ Y_e = Y_e(\alpha) \end{cases} \tag{3}$$

The EME model, similar to the linearized model, derived from EM of the nonlinear system can be regarded as a real-time Taylor expansion model, as described below:

$$\begin{cases} \dot{X} = A(\alpha)(X - X_e(\alpha)) + B(\alpha)(U - U_e(\alpha)) \\ Y = Y_e(\alpha) + C(\alpha)(X - X_e(\alpha)) + D(\alpha)(U - U_e(\alpha)) \\ \alpha = p(X, U) \end{cases} \tag{4}$$

where $A(\alpha)$, $B(\alpha)$, $C(\alpha)$, and $D(\alpha)$ are parameterized Jacobian linearization system matrices, p is a mapping relationship between α and system variables X and U.

2.2. Model Identification Method and Analysis of Simulation Results

In this part, the identification method and the superiority of the EME model will be introduced with a two-spool turbofan engine. A detailed description of the engine is given in Section 4.1. The engine runs under standard atmospheric conditions. Under the premise that the inlet guide vane (IGV) and nozzle area remains constant, the engine can be regarded as an SI nonlinear system. The unique input is fuel flow, q_{mf}. The state variables are high pressure turbine rotor speed n_h and fan rotor speed n_l. To obtain an accurate EME model, the fuel flow needs to be composed of several step signals, as shown in Figure 1a. The corresponding signals of n_h and n_l are shown in Figure 1b. The data have been standardized.

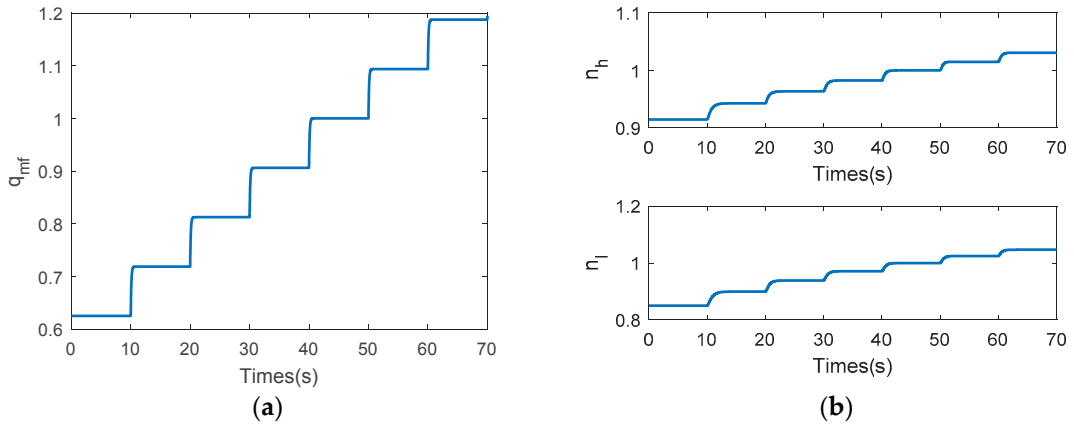

Figure 1. (**a**) Command signal of q_{mf}; (**b**) signals of n_h and n_l.

Then, a two-step method of "dynamic and static" type is carried out for the EME model parameter identification. And the identification process is made up of three parts:

1. Define the scheduling variable α

For the equilibrium family (2), there are n equations with n + 1 variables so that the scheduling variable α is defined as a one-dimension vector. According to [4], the scheduling variable α can be specified as the input, the state variable of the nonlinear system or be derived from the orthogonal expansion, for which the modeling accuracy is the only difference. In this section, for the convenience of modeling, the fuel flow q_{mf} is selected as the scheduling variable.

2. Identify parameters of EM

EM (3) is obtained by fitting steady state points of the nonlinear system, as shown in Figure 2. In general, EM can be expressed as polynomials by the scheduling variable α.

$$Z_e = \sum_{i=0}^{n} k_i \alpha^i \tag{5}$$

where Z_e represents the input vector, the state vector, or the output vector, k_i is the polynomial coefficient, n is the polynomial order, which is of order four in this paper.

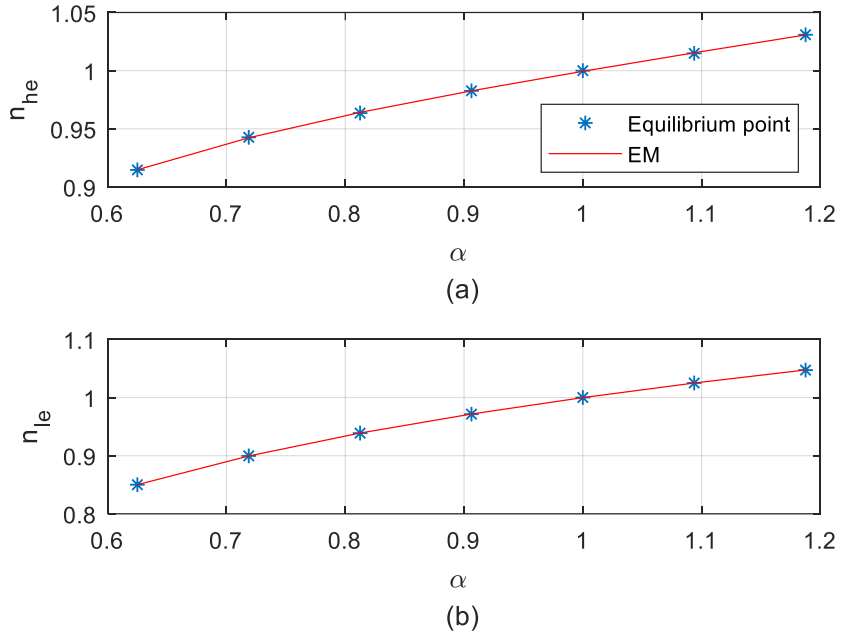

Figure 2. (a) EM of n_{he}; (b) EM of n_{le}.

3. Identify parameters of parameterized Jacobian linearization system matrices

The parameterized Jacobian linearization system matrices are also expressed as polynomials like the Equation (5), as shown below:

$$\dot{X} = \sum_{j=0}^{n_A} a_j \alpha^j (X - X_e(\alpha)) + \sum_{k=0}^{n_B} b_k \alpha^k (U - U_e(\alpha)) \tag{6}$$

The polynomial order is determined by the degree of nonlinearity of the system, which is two orders in this part.

After calculating derivatives of the state vector, namely, $\dot{X}$, the parameters of parameterized Jacobian linearization system matrices are identified using the data in the red box of Figure 3 by the linear regression.

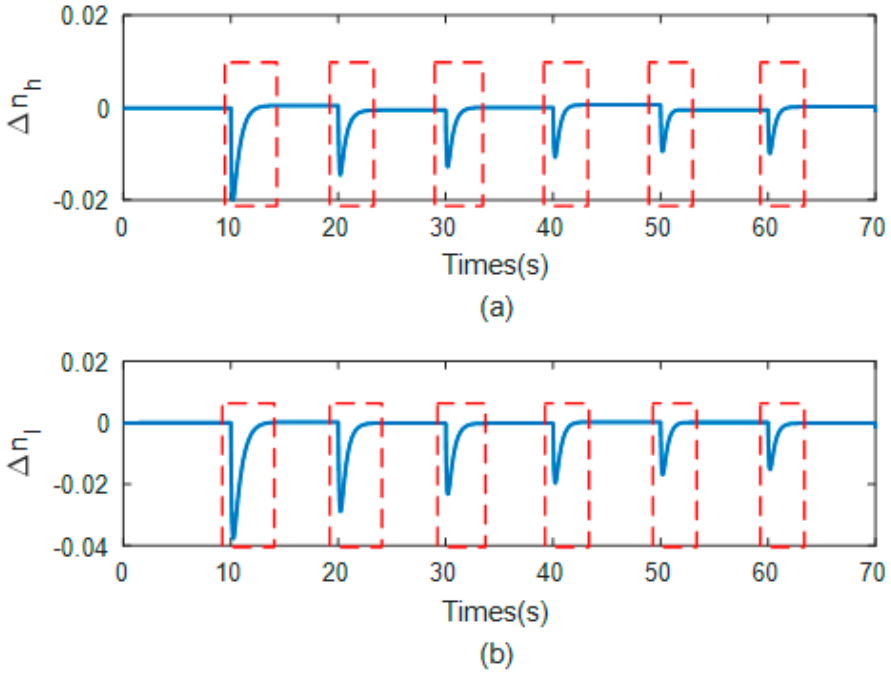

Figure 3. Deviation variables of (**a**) n_h and (**b**) n_l.

Thus far, parameters of EMs and parameters of parameterized Jacobian linearization system matrices have been obtained. Figure 4 indicates the superior capability of the EME model to represent the engine's behaviors no matter in steady state and transient. The maximum errors of n_h and n_l are just 0.096%and 0.097%, respectively, which fully meets the requirements of system simulation or control.

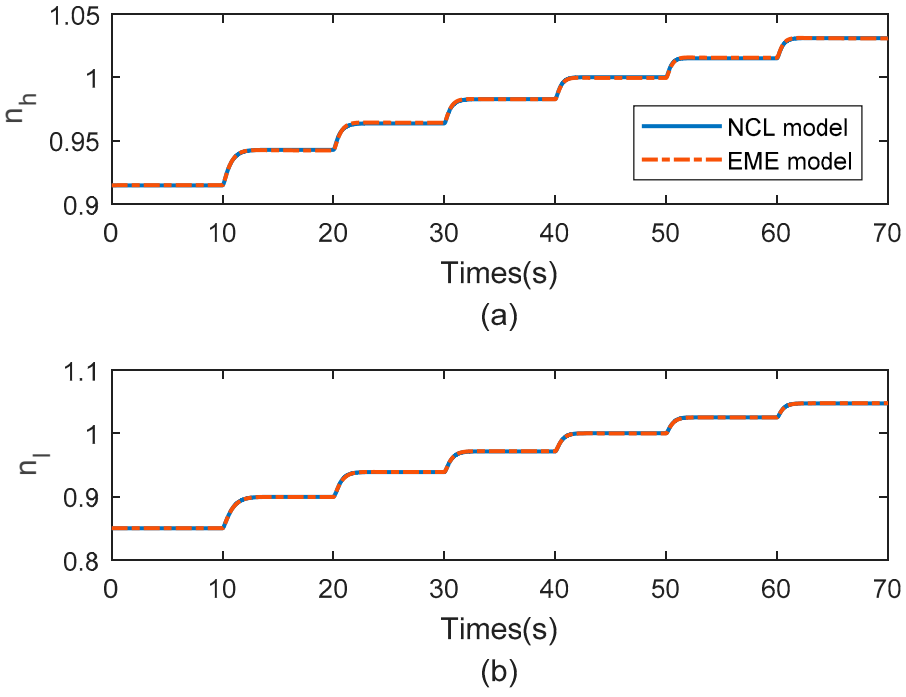

Figure 4. State responses (**a**) n_h and (**b**) n_l of the EME model and the engine.

2.3. Discussion on the EME Model Deficiency

For an SI system, the scheduling variable α_1 and state variable x_1 form an EM of AB' in two-dimensional space. And the corresponding EME model can guarantee the stability of calculation on AB', as shown in Figure 5. When the input variable of the system becomes two-dimensional, there is another scheduling variable α_2 for the construction of EM that is a surface in the three-dimensional space. Although the parameter identification of the EM can be completed under the condition that there are enough stable points, the method of least square identification of dynamic matrices with constraints can only ensure the calculation stability of the EME model on a single trajectory AC'. When the running point of the system deviates too far from the given trajectory or the motion direction is inconsistent with the given trajectory, the divergence of the model calculation results may occur.

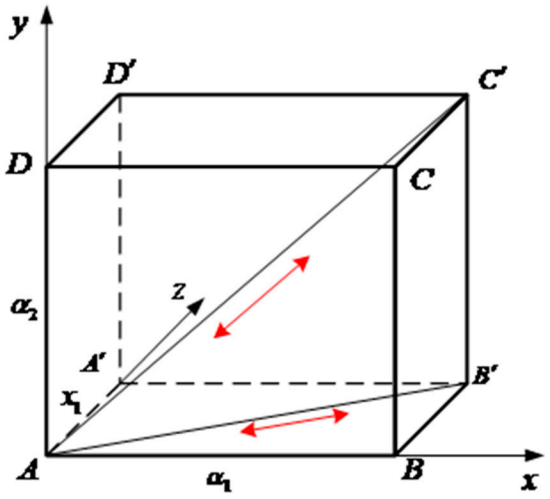

Figure 5. A schematic diagram of dimension expansion of the EM.

The success of SI EME models urges us to consider whether it is possible to use the prior knowledge of gas turbine to compress the high-dimensional EM into one-dimensional EM to ensure the accuracy and stability of an MI-EME model for the special object of a gas turbine.

3. The Conception of the CEME Model

The range of aero-engine flight altitude and flight speed varies widely, which results in a large change in the total inlet temperature and pressure of the engine. An SI-EME model cannot meet the needs of practical applications. In this section, a corrected equilibrium manifold expansion (CEME) model, a novel MI-EME model, is proposed by integrating the prior knowledge of the gas turbine.

3.1. Corrected Equilibrium Manifold

According to the common working principle of the gas turbine components, there is only one determinate component performance and overall engine performance in a steady state of the aero-engine. A line is made up of all these points, which is called the operating line. The operating line is generally measured by experiments and then marked on the characteristic diagram of the engine compressor and turbine [16], as shown in Figure 6 where A, B, C, and D are operating points. However, different operating lines are obtained under different EICs. It is impossible to obtain all the operating lines by experiments alone. The similarity theory is carried out to nondimensionalize engine variables, like gas flow, rotor speed, temperature, and pressure, to make the engine in a similar state to solve such a problem. It is concluded that nondimensionalized engine variables in a similar state, also called

a similar parameter, remain constant no matter how flight conditions, ambient conditions, and engine rotor speed change, like Equation (7) that is the reduced fuel flow:

$$\frac{q_{mf,1}}{p^*_{a,1}\sqrt{T^*_{a,1}}} = \frac{q_{mf,2}}{p^*_{a,2}\sqrt{T^*_{a,2}}} = constant \tag{7}$$

where subscript "1" and "2" represent the different EICs, p^*_a is the engine inlet total pressure and T^*_a is the engine inlet total temperature.

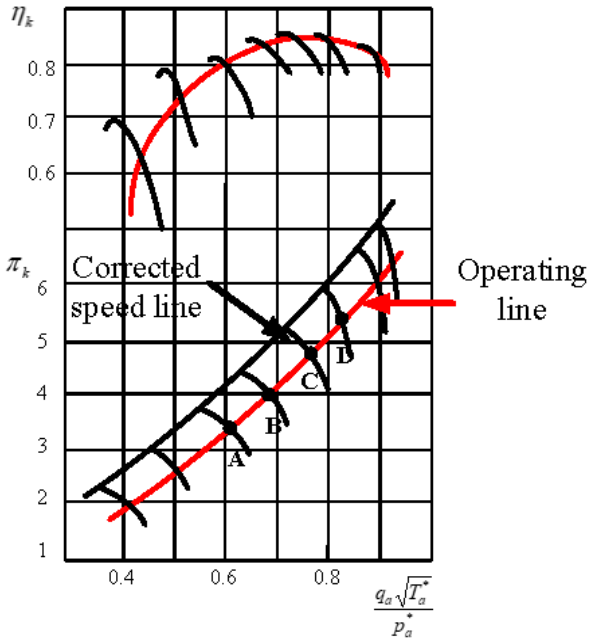

Figure 6. Compressor characteristic curves.

In other words, obtaining the engine state at one EIC is equivalent to obtaining the engine state at all EICs. Moreover, according to the reference [17], when an engine works in a similar state, both its steady-state characteristics and its dynamic characteristics are similar. Such an important conclusion has allowed similarity theory to become a general theory in the field of engine design [18] and modeling [19]. It is also an important theoretical basis for the CEME model.

For an SI-EME model, the input is usually specified as engine fuel flow due to its leading role. Thus, p^*_a and T^*_a need to be forced to remain constant to not affect the match between the EME model and the engine. For the SI-EME model, compared with Equation (3) the complete EM should be described as:

$$\begin{cases} X_e = X_e(\alpha) \\ U_e = U_e(\alpha) \\ Y_e = Y_e(\alpha) \end{cases} \\ subject\ to \\ p^*_a = constant \\ T^*_a = constant \tag{8}$$

Once p^*_a and T^*_a change, the aero-engine will form an unknown EM. It assumes that there is arbitrary equilibrium point A $(X_{e,A}, U_{e,A}, Y_{e,A}, \alpha_{e,A})$ on the unknown EM under the EIC $\left(p^*_{a,A}, T^*_{a,A}\right)$, as shown in Figure 7. The following equations must be similar to Equation (7) for equilibrium point A

and a certain equilibrium point B $(x_{e,B}, u_{e,B}, y_{e,B}, \alpha_{e,B})$ on the known EM under the fixed EIC $\left(p^*_{a,B}, T^*_{a,B}\right)$ based on the similarity theory:

$$\begin{cases} f_1\left(x_{e,A}, p^*_{a,A}, T^*_{a,A}\right) = f_1\left(x_{e,B}, p^*_{a,B}, T^*_{a,B}\right) = constant \\ f_2\left(u_{e,A}, p^*_{a,A}, T^*_{a,A}\right) = f_2\left(u_{e,B}, p^*_{a,B}, T^*_{a,B}\right) = constant \\ f_3\left(y_{e,A}, p^*_{a,A}, T^*_{a,A}\right) = f_3\left(y_{e,B}, p^*_{a,B}, T^*_{a,B}\right) = constant \\ f_4\left(\alpha_{e,A}, p^*_{a,A}, T^*_{a,A}\right) = f_4\left(\alpha_{e,B}, p^*_{a,B}, T^*_{a,B}\right) = constant \end{cases} \tag{9}$$

where f_1, f_2, f_3, and f_4 are similarity equations.

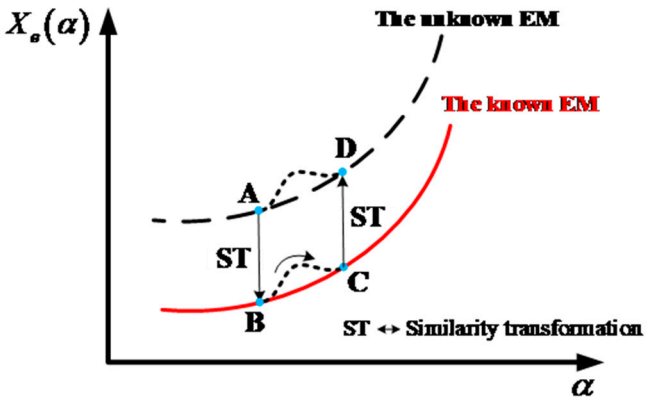

Figure 7. Computational process of CEME model.

Transform Equation (9) to:

$$\begin{cases} x_{e,B} = F_1\left(x_{e,A}, p^*_{a,A}, T^*_{a,A}, p^*_{a,B}, T^*_{a,B}\right) \\ u_{e,B} = F_2\left(u_{e,A}, p^*_{a,A}, T^*_{a,A}, p^*_{a,B}, T^*_{a,B}\right) \\ y_{e,B} = F_3\left(y_{e,A}, p^*_{a,A}, T^*_{a,A}, p^*_{a,B}, T^*_{a,B}\right) \\ \alpha_{e,B} = F_4\left(\alpha_{e,A}, p^*_{a,A}, T^*_{a,A}, p^*_{a,B}, T^*_{a,B}\right) \end{cases} \tag{10}$$

Then substitute them into Equation (8):

$$\begin{cases} F_1\left(x_{e,A}, p^*_{a,A}, T^*_{a,A}, p^*_{a,B}, T^*_{a,B}\right) = x_e\left(F_4\left(\alpha_{e,A}, p^*_{a,A}, T^*_{a,A}, p^*_{a,B}, T^*_{a,B}\right)\right) \\ F_2\left(u_{e,A}, p^*_{a,A}, T^*_{a,A}, p^*_{a,B}, T^*_{a,B}\right) = u_e\left(F_4\left(\alpha_{e,A}, p^*_{a,A}, T^*_{a,A}, p^*_{a,B}, T^*_{a,B}\right)\right) \\ F_3\left(y_{e,A}, p^*_{a,A}, T^*_{a,A}, p^*_{a,B}, T^*_{a,B}\right) = y_e\left(F_4\left(\alpha_{e,A}, p^*_{a,A}, T^*_{a,A}, p^*_{a,B}, T^*_{a,B}\right)\right) \\ subject\ to \\ p^*_{a,B} = constant \\ T^*_{a,B} = constant \end{cases} \tag{11}$$

Although the equilibrium point A is on the unknown EM, it can also be transferred to the known EM by similarity transformation under the condition that the EIC corresponding to the unknown EM is known. In other words, the known and unknown EMs can transform into each other based on the similarity theory. From this, we can conclude that in the process of multi-input expansion of EM, a one-dimensional EM can be combined with similar equations to integrate the EIC into the EM to obtain a high-dimensional EM. Since similarity equations are the essential property of the gas turbine, the new equilibrium manifold, called corrected equilibrium manifold (CEM), formed by the combination of the one-dimensional EM and similarity equations are more in line with the general law of gas turbine performance change. Compared with the high-dimensional EM by polynomial fitting, the CEM reduces the influence of fitting error on the MI EME model due to the introduction of nonlinear equations. Furthermore, the modeling data for one-dimensional EM is enough to identify

the high-dimensional EM, and even it is not necessary to keep the EIC constant when establishing one-dimensional EM.

3.2. CEME Model Structure and Computation Process

The above section mainly focuses on the definition of CEM and proves that the unknown EMs under different EICs can transform into the known EM under the fixed EIC based on the similarity theory. In this section, the structure of the CEME model, computational process and requirements for CEME modeling are discussed.

According to the similarity theory, when an engine works in a similar state, both its steady-state characteristics and its dynamic characteristics are similar. It means that the dynamic process on the unknown EM is in the same similar state as that on the known EM. Thus, according to the inlet condition of the engine, the working point on the unknown EM is transferred to the known EM in the accordance with EIC, and then its dynamic process can be calculated by using the known EME model. The above process can be regarded as a "forward process" of similar transformation like the process from A to B shown in Figure 7. Since the calculation result of the known EME model is a representation of the dynamic process on the known EM, the final result also needs a similar transformation to transfer it back to the unknown EM. Such a process can be regarded as a "backward process" of similar transformation like the process from C to D. Through the above process, the EIC can be incorporated into the EME model as inputs. Since the SI-EME model can guarantee global computational stability, the new model can still guarantee global computational stability. The new EME model is called a corrected equilibrium manifold expansion (CEME) model in this paper. The model structure is described as below:

$$\begin{cases} \dot{x}_{ceme} = A(\alpha)(x_{\text{ceme}} - x_e(\alpha)) + B(\alpha)(u_{ceme} - u_e(\alpha)) \\ y_{ceme} = y_e(\alpha) + C(\alpha)(x_{ceme} - x_e(\alpha)) + D(\alpha)(u_{ceme} - u_e(\alpha)) \\ \alpha = p_{FSC}\left(x, u, p^*_{a,fixed}, T^*_{a,fixed}, p^*_{a,input}, T^*_{a,inpout}\right) \\ x_{ceme} = f_{FSC,1}\left(x, p^*_{a,fixed}, T^*_{a,fixed}, p^*_{a,input}, T^*_{a,input}\right) \\ u_{ceme} = f_{FSC,2}\left(u, p^*_{a,fixed}, T^*_{a,fixed}, p^*_{a,input}, T^*_{a,input}\right) \\ y = f_{BSC}\left(y_{ceme}, p^*_{a,fixed}, T^*_{a,fixed}, p^*_{a,input}, T^*_{a,input}\right) \end{cases} \tag{12}$$

$$\begin{aligned} &subject\ to \\ &p^*_{a,fixed} = constant \\ &T^*_{a,fixed} = constant \end{aligned}$$

where $p^*_{a,fixed}$ and $T^*_{a,fixed}$ represent the EIC corresponding to the known EM, $p^*_{a,input}$ and $T^*_{a,input}$ are inputs of the CEME model, p_{FSC} is a mapping including forward similarity calculation, $f_{FSC,1}$ and $f_{FSC,2}$ are forward similarity calculation functions and f_{BSC} is a backward similarity calculation function.

By observing the structure of the CEME model, we can know that the introduction of similarity equations does not change the polynomial coefficients in the model like parameterized Jacobian linearization system matrices and EM. It means that the existing SI-EME model identification method is also effective for the CEME model. Moreover, the requirements for modeling data is reduced. Steady-state operating points of the engine are required to be under the same EIC in the existing SI-EME model identification method. However, in our proposed method steady-state operating points under different EICs can be used for modeling. Hence, the CEME model can be built using engine historical data rather than additional experiments.

4. CEME Modeling Experiment

4.1. Turbofan Engine Model

The identification procedure of the CEME model is conducted by a two-spool turbofan engine with a low bypass ratio and a 4 kN gross thrust that is a nonlinear component level (NCL) model built based on modular modeling method with reference of the paper [10]. The turbofan engine included an atmospheric module, fan, compressor, combustor module, and high pressure and low pressure turbines connected to two spools and developed dynamic modules for each part of the turbofan engine, as shown in Figure 8. The dynamic behavior of each module is represented by a series of equations including the thermodynamic relations, mass, momentum, and energy balance. The mass and momentum balance equations are used in a one-dimensional differential form based on the hypothesis that the section duct of each module is constant and the efficiency coefficient and flow coefficient are described in the form of general characteristic maps and look-up tables.

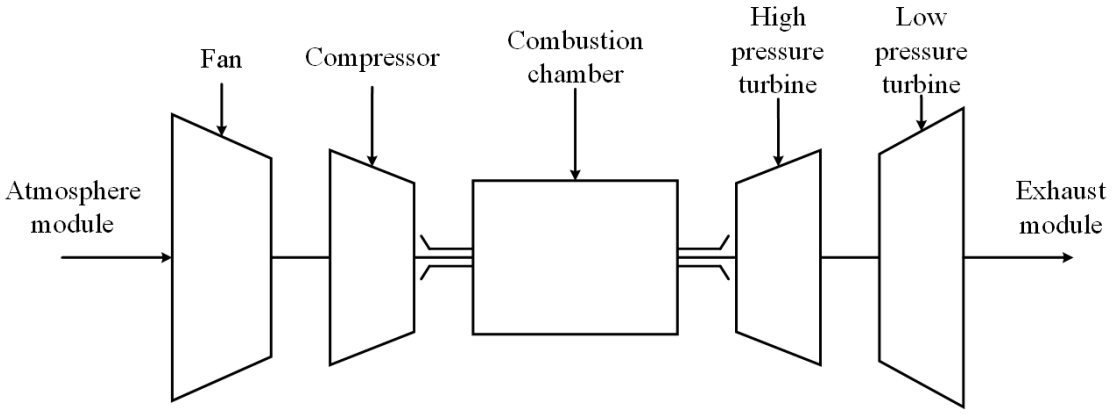

Figure 8. Schematic of a turbofan engine.

According to a mechanical viewpoint, the fluid within components is considered an ideal gas and the specific heat in each module is the mean value at constant pressure and volume calculated by the fluid composition and the temperature between modules input and output, by which the model accuracy is not significantly affected, but both the model complexity and the calculation time are considerably reduced. Additionally, equations representing the dynamic balance of shafts and rotating masses of the components connected to them are also used. It should be noted that thermodynamic transformation equations are calculated in stationary form because the shaft inertia is so great that the fluid thermal inertia can be neglected. The simulation of the turbofan engine was conducted by integrating the differential equations and solving the static equations with the variable values calculated at each time instant.

4.2. Structure of CEME Model

The fan rotor speed n_l and high pressure turbine rotor speed n_h are determined as states of the CEME model. Inputs fuel flow q_{mf}, inlet total temperature T_a^* and inlet total pressure p_a^* are inputs of the CEME model. All measurements corresponding to the engine gas path including temperature, pressure, and rotor speed, can be considered as outputs of the CEME model. This paper selects the high pressure turbine outlet total temperature T_{35}^* and the low pressure turbine outlet total pressure p_4^* are selected as outputs for the CEME model validation. q_{mf}, T_a^*, and p_a^* are selected as the scheduling variables. Then, a complete CEME model can be described as:

$$\begin{cases} \dot{n}_h = a_{11}(\alpha)(\frac{\sqrt{T^*_{a,fixed}}}{\sqrt{T^*_a}}n_h - n_{he}(\alpha)) + a_{12}(\alpha)(\frac{\sqrt{T^*_{a,fixed}}}{\sqrt{T^*_a}}n_l - n_{le}(\alpha)) \\ \dot{n}_l = a_{21}(\alpha)(\frac{\sqrt{T^*_{a,fixed}}}{\sqrt{T^*_a}}n_h - n_{he}(\alpha)) + a_{22}(\alpha)(\frac{\sqrt{T^*_{a,fixed}}}{\sqrt{T^*_a}}n_l - n_{le}(\alpha)) \\ T^*_{35} = \frac{T^*_a}{T^*_{a,fixed}}(c_{11}(\alpha)(\frac{\sqrt{T^*_{a,fixed}}}{\sqrt{T^*_a}}n_h - n_{he}(\alpha)) + c_{12}(\alpha)(\frac{\sqrt{T^*_{a,fixed}}}{\sqrt{T^*_a}}n_l - n_{le}(\alpha))) \\ p^*_4 = \frac{p^*_a}{p^*_{a,fixed}}(c_{21}(\alpha)(\frac{\sqrt{T^*_{a,fixed}}}{\sqrt{T^*_a}}n_h - n_{he}(\alpha)) + c_{22}(\alpha)(\frac{\sqrt{T^*_{a,fixed}}}{\sqrt{T^*_a}}n_l - n_{le}(\alpha))) \\ \alpha = \frac{p^*_{a,fixed}\sqrt{T^*_{a,fixed}}}{p^*_a\sqrt{T^*_a}}q_{mf} \end{cases} \quad (13)$$

$$\begin{aligned} &subject\ to \\ &p^*_{a,fixed} = 101.3kPa \\ &T^*_{a,fixed} = 288.15K \end{aligned}$$

where $p^*_{a,fixed}$ and $T^*_{a,fixed}$ are the given EIC corresponding to the known EM.

4.3. CEME Modeling and Verification

4.3.1. Generation of the I/O Data

From Equation (13), we can know that if the inputs of p^*_a and T^*_a are equal to $p^*_{a,fixed}$ and $T^*_{a,fixed}$ the CEME model is equivalent to an SI-EME model. This means that the existing EME identification method is still suitable to the CEME identification. Furthermore, because of similarity theory, the data under any EIC can be used for CEME modeling as long as converted data, namely, the converted fuel flow, is still a multiple-step signal, which is equivalent to relaxing the requirements for modeling data. Compared with the fixed EIC, more general experimental data are given. Thus, engine inlet total temperature and total pressure command signals are shown in Figure 9a, which are normalized by the reference value of 288.15 K and 101.325 kPa. The fuel flow command signal is shown in Figure 9b, where the fuel flow is normalized by the reference value of 160 L/h. Other system variables, like temperature and pressure, are normalized by reference values corresponding to engine conditions at 160 L/h fuel flow as well.

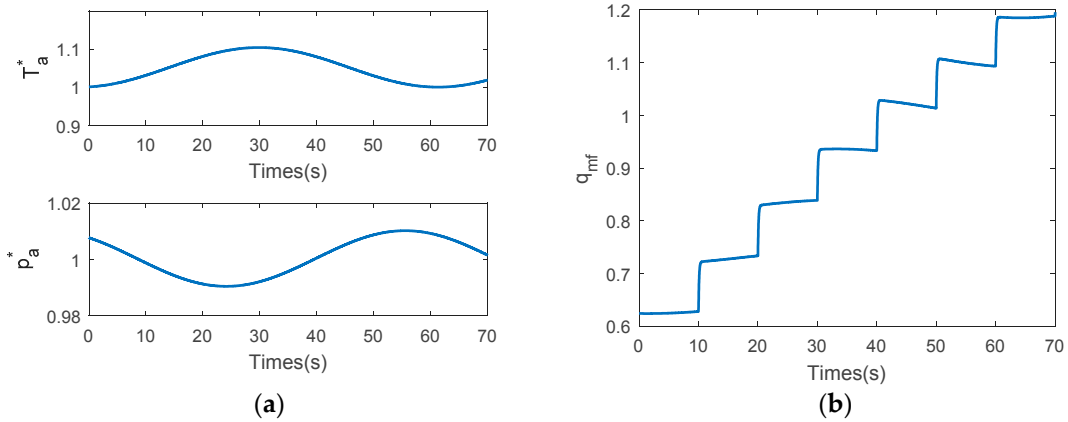

Figure 9. (**a**) Signal of EIC; (**b**) command signal of fuel flow.

4.3.2. CEME Modeling Procedure

Before modeling, it is necessary to convert all the data to the state corresponding to $p^*_{a,fixed}$ and $T^*_{a,fixed}$ to ensure that an accurate EM can be obtained. Then, all modeling steps are the same as that described in Section 2.2. Polynomials of EMs and parameterized Jacobian linearization system matrices are still 4 orders and 2 orders, respectively. In addition, this paper enumerates "percentage of

compliance (*PC*)" index, "mean error percentage (*MeanEP*)" index and "maximum error percentage (*MaxEP*)" index to evaluate the CEME model performance. The *PC*, *MeanEP* and *MaxEP* indices are defined as Equations (14)–(16), respectively:

$$PC = \left(1 - \frac{\|Y - \hat{Y}\|}{\|Y - \overline{Y}\|}\right) \times 100 \tag{14}$$

$$MeanEP = \sum_{i=1}^{D} \left(\left| \frac{Y(i) - \hat{Y}(i)}{Y(i)} \right| \times 100 \right) / D \tag{15}$$

$$MaxEP = \max_{D} \left(\left| \frac{Y(i) - \hat{Y}(i)}{Y(i)} \right| \times 100 \right) \tag{16}$$

where Y and $\hat{Y}$ represent the vectors of the desired and estimated engine outputs, respectively, and $\overline{Y}$ represents the mean value of Y. $\|\cdot\|$ represents the Euclidean norm and Y denotes the dimension of Y.

The final simulation result displayed in Figure 10 indicates the superior capability of the CEME model to represent behaviors of the NCL model. More detailed information has been shown in Table 1, which shows that *PC* exceeds 98 and *MaxEP* does not exceed 0.4%.

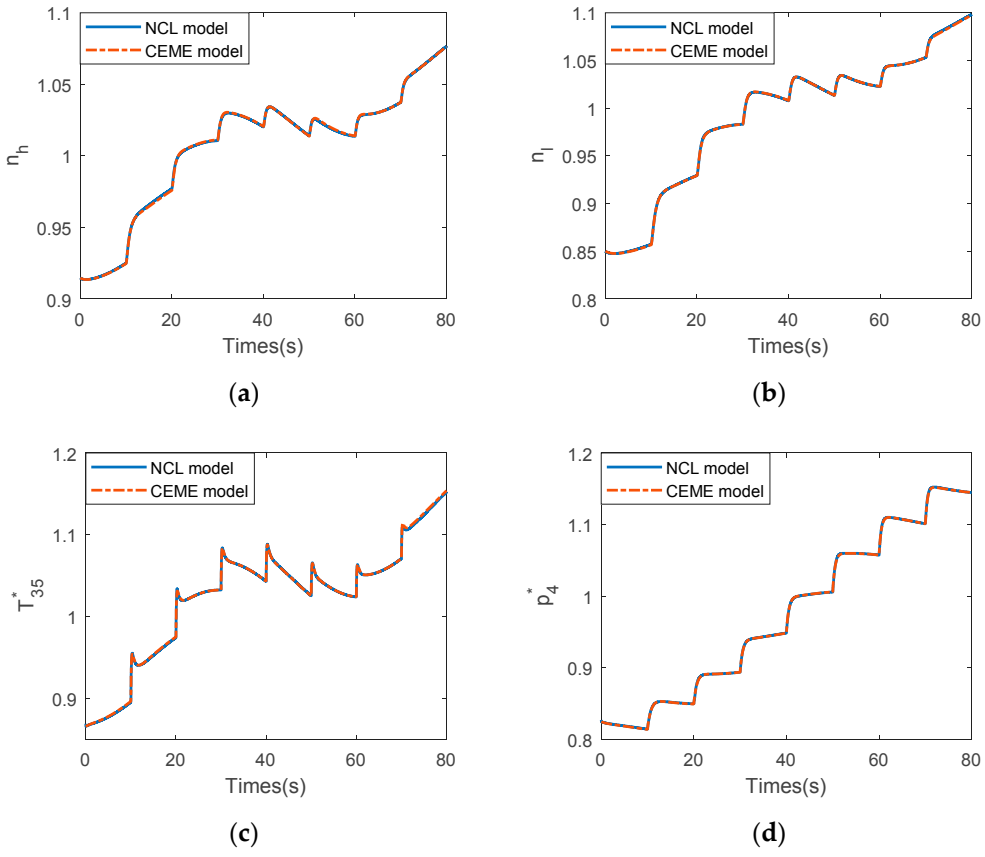

Figure 10. State responses (**a**) n_h, (**b**) n_l, (**c**) T^*_{35} and (**d**) p^*_4 of the CEME model and the NCL model.

Table 1. Simulation results on training data set.

Variables	n_h	n_l	p^*_4	T^*_{35}
PC (%)	98.91	99.49	98.91	99.73
MaxEP (%)	0.171	0.130	0.388	0.353
MeanEP (%)	0.037	0.030	0.057	0.028

4.3.3. CEME Model Verification

It should be noted that in the process of building the CEME model, the EIC is not involved in determining the structure parameters of the CEME model, but only incorporated into the CEME model in the form of similar parameters. Therefore, it is necessary to demonstrate whether the CEME model is in very good accordance with the NCL model in both steady and dynamic aspects when the EIC changes independently. A test uses a combination of gradient signal and step signal as the EIC signal meanwhile the fuel flow is kept at 160 L/h, as shown in Figure 11. The simulation results displayed in Figure 12 indicate its capability to represent the engine's behaviors. Compared with Tables 1 and 2, three indices are unchanged, which further proves the effectiveness of the proposed method. The computing time of the CEME model is 40.86 s and that of the NCL model is 67.29 s, which indicates the CEME model with simpler model structure gets faster computing speed than the physical-based NCL model.

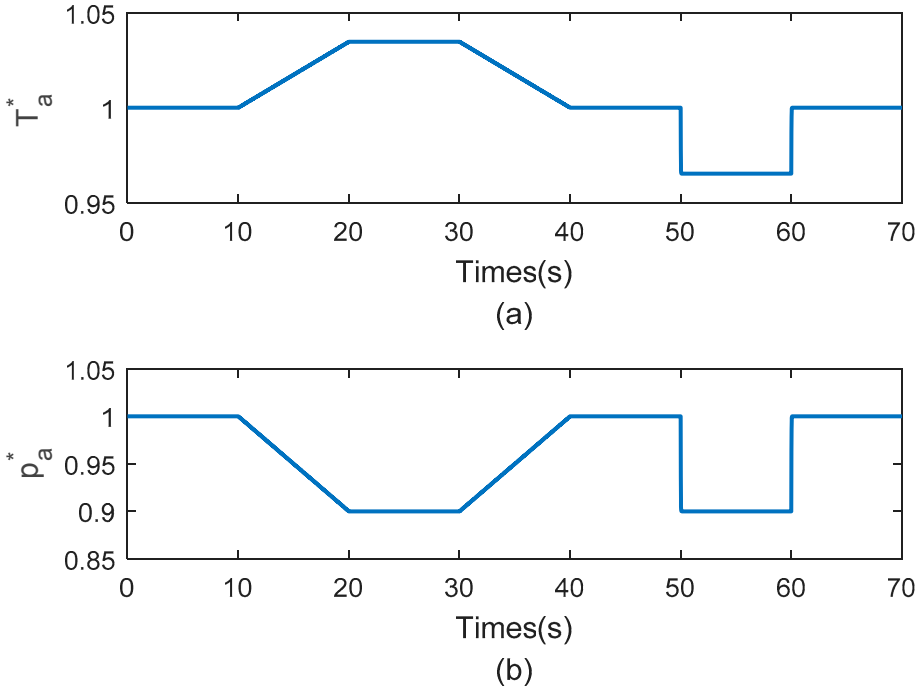

Figure 11. Command signals of (a) T_a^* and (b) p_a^*.

Table 2. Simulation results on test data set.

Variables	n_h	n_l	p_4^*	T_{35}^*
PC (%)	97.51	97.08	98.29	99.23
MaxEP (%)	0.203	0.634	0.235	0.206
MeanEP (%)	0.028	0.053	0.033	0.022

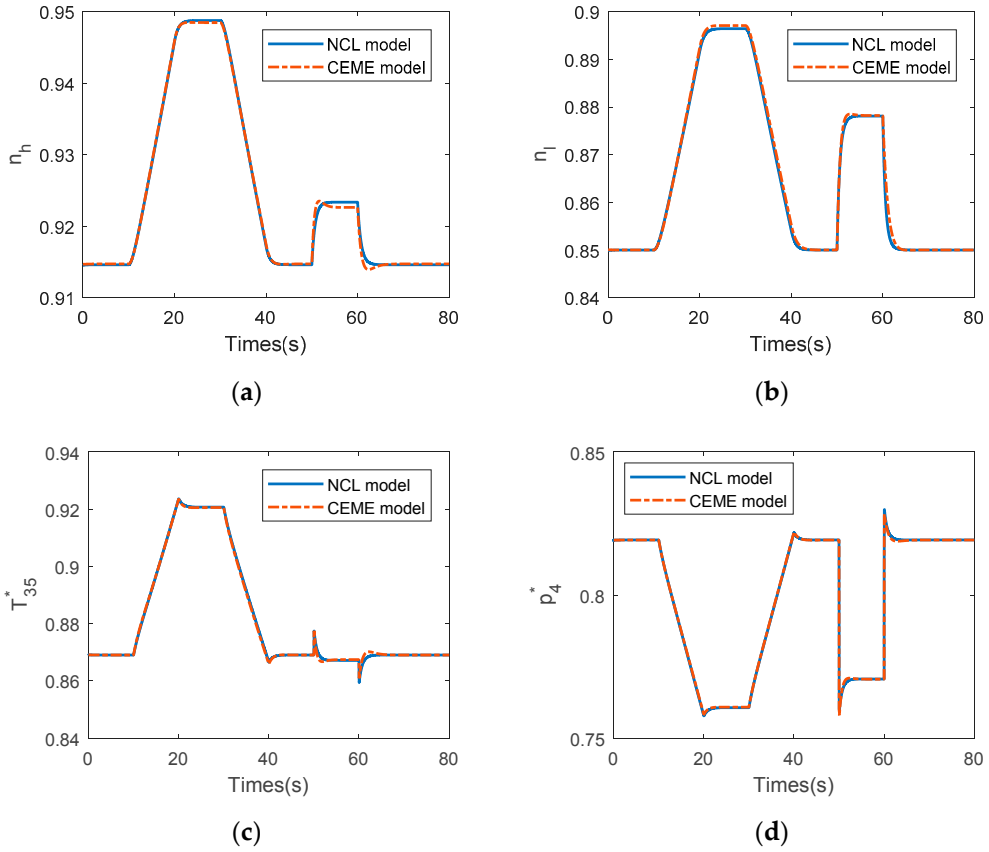

Figure 12. Dynamical behaviors (**a**) n_h, (**b**) n_l, (**c**) T^*_{35} and (**d**) p^*_4 of the CEME model and the NCL model.

5. Comparative Experiment

In this section, the performance of the CEME model built in the above section in predicting the dynamic and static behaviors of the aero-engine is evaluated against two MI-EME models identified by the existing identification method. The MI-EME model has two inputs, namely, q_{mf} and T^*_a. EMs of two MI-EME models are both fourth-order polynomials. Parameterized Jacobian linearization system matrices of them are one order and two order polynomials, respectively. All steady state points, shown in Figure 13, are used for identifying the EM, and the dash-dot line shown in Figure 13 is used for identifying the parameterized Jacobian linearization system matrices. The scheduling variables of MI-EME models are determined as q_{mf} and T^*_a. We will demonstrate the superiority of the CEME model than MI-EME models from three aspects including the implementability of modeling, model accuracy, and model calculation stability.

5.1. Analysis of Implementability

From the perspective of data volume, the proposed method effectively reduces the workload of modeling. Taking the two input EME model built in this section as an example, the EM is a two-dimensional surface. It needs enough steady state points like Figure 13 which has 64 steady state points to get a relatively large EM by using the existing identification method. Additionally, if the engine inlet total pressure is also determined as the EME model input, the number of the steady state points will increase exponentially. However, based on the proposed method, only one step curve in Figure 13, that is, eight steady state points are needed, and the others are obtained by using similarity equations. Hence, the proposed method effectively reduces the workload of modeling.

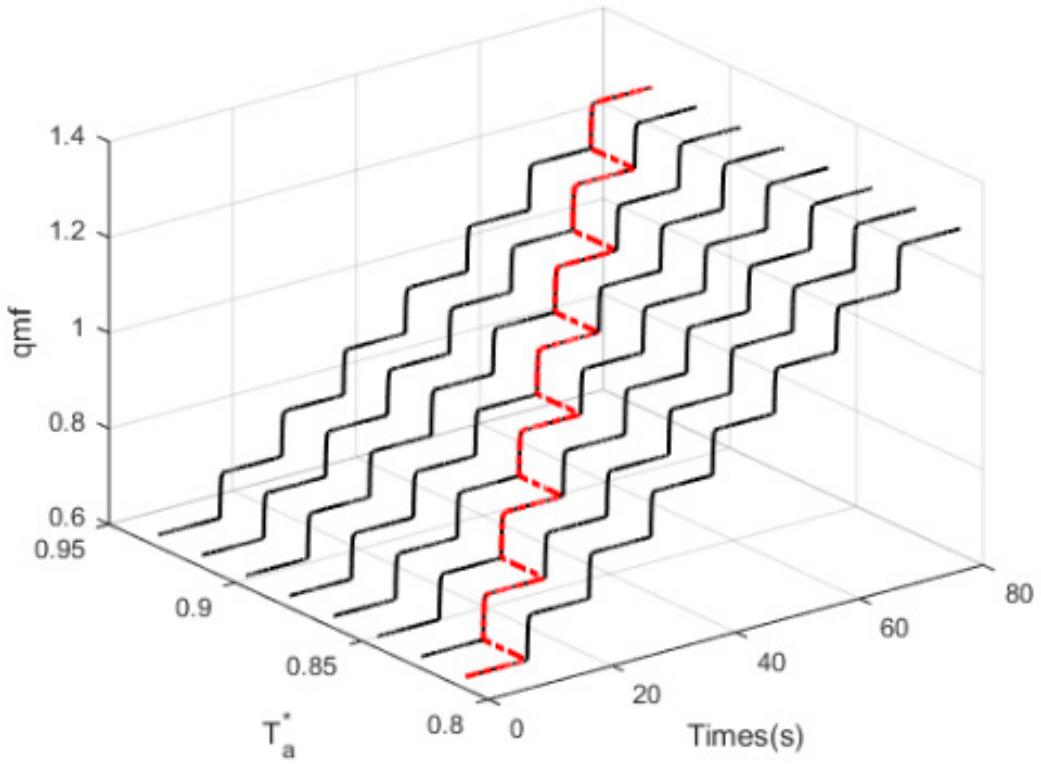

Figure 13. Command signals of q_{mf} and T_a^* in the training set.

From the perspective of identifying parameters of parameterized Jacobian linearization system matrices, it is easier to implement the proposed method. The purpose of using step signals is to fully excite the dynamic characteristics of the system. For an MI-EME model, the parameterized Jacobian linearization system matrices are polynomials composed of multiple scheduling variables. Due to the nature of the MI-EME model being a nonlinear model, the superposition principle of a linear system is not suitable for the EME model. Thus, it is necessary to ensure the synchronization of step signals to obtain accurate model parameters. In the CEME modeling process, the CEME model degenerates to an SI model so it avoids the above harsh modeling requirements.

Finally, from the perspective of practical application, it is very difficult to control the EIC for a real gas turbine, let alone force the EIC to be a step signal. On the contrary, such a restriction on EIC has been relaxed by using the proposed method, which has been fully discussed in Section 4.

5.2. Performance Analysis of Examined Models

Figure 14a–d illustrate the performances of three models in estimating the dynamic and static behaviors of the aero-engine against the training data. More details are outlined in Table 3. This indicates that although the amount of modeling data of the CEME model is just one eighth of that of the MI-EME models, the CEME model has almost the same good performance in estimating the dynamic and static behaviors of the aero-engine as two MI-EME models, except for *MaxEPs* of T_{35}^* and p_4^*. However, they are both less than 1%, which meets the needs of control or fault diagnosis.

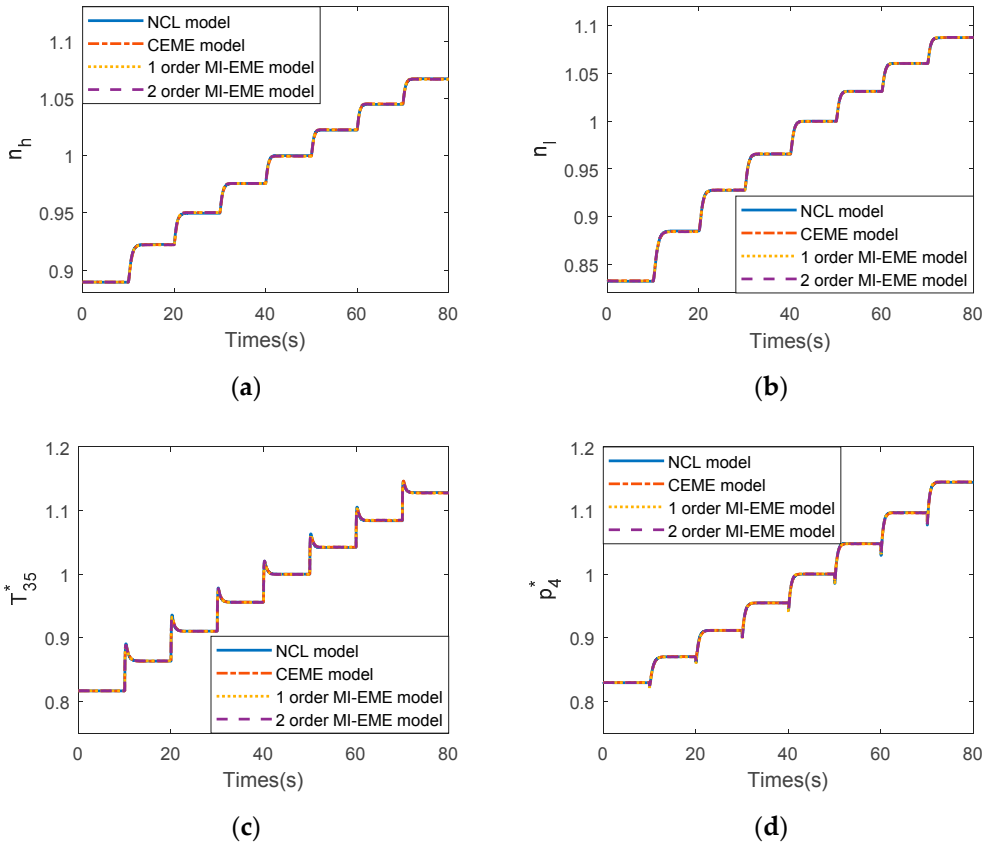

Figure 14. (**a**) n_h variations in training set; (**b**) n_l variations in training set; (**c**) T^*_{35} variations in training set; (**d**) p^*_4 variations in training set.

Table 3. Performance comparison of the examined models.

Variables	Model	PC (%)	MaxEP (%)	MeanEP (%)
n_h	CEME	99.30	0.235	0.036
	1-order MI-EME	99.42	0.105	0.029
	2-order MI-EME	99.43	0.097	0.029
n_l	CEME	99.43	0.097	0.029
	1-order MI-EME	99.59	0.194	0.032
	2-order MI-EME	99.56	0.196	0.033
p^*_4	CEME	99.57	0.190	0.033
	1-order MI-EME	99.56	0.752	0.040
	2-order MI-EME	99.49	0.681	0.045
T^*_{35}	CEME	99.52	0.335	0.042
	1-order MI-EME	99.56	0.784	0.041
	2-order MI-EME	99.63	0.358	0.033

For studying the computational stability of the examined models, another test is carried out. The inputs of models are shown in Figure 15a, where there are different signal types to reflect the running state of the engine under different operating conditions. The simulation results are shown in Figure 15b, from which we can see that the calculation results in two MI-EME models diverging at 80–90 s. Comparatively, the CEME model runs stably throughout the whole process. The calculation instability of two MI-EME models is mainly caused by the improper dynamic parameter fitting of

the model. Restricted by the existing identification method, an MI-EME model theoretically only guarantees the model stability in one direction, but not the global model stability, which is summarized as the insufficient generalization ability of the model, or called overfitting. The overfitting will be worse and worse with the increase of the order of parameterized Jacobian linearization system matrices. This is why the two-order MI-EME model diverges earlier than the one-order MI-EME model. For the CEME model, on the premise of ensuring the model stability along one direction, the calculation along other directions is completed by similar transformation, thus ensuring the global stability.

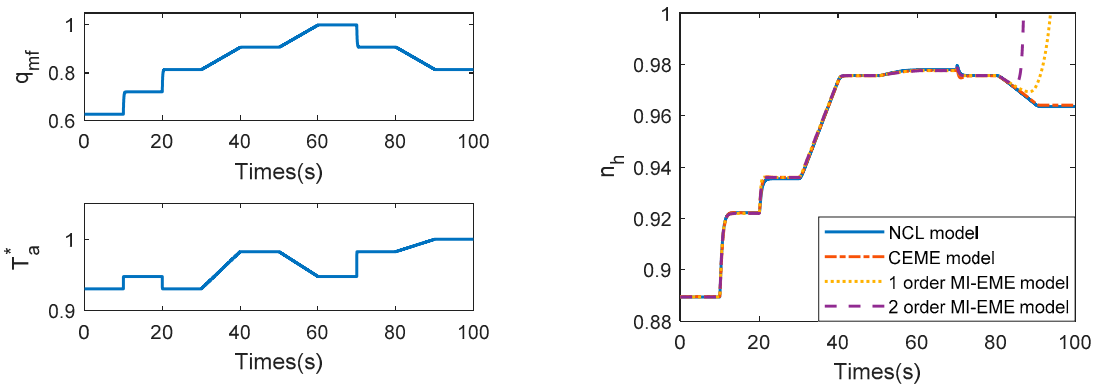

(**a**) (**b**)

Figure 15. (**a**) Command signals of q_{mf} and T_a^* in test set; (**b**) n_h variations in test set.

6. Conclusions

The EME modeling procedure for aero-engines is rational and time-saving. However, the multiple-input EME model built by the existing identification method has problems of calculation instability and difficulties in engineering applications. For solving problems, this paper proposed a corrected EME model. According to the theoretical analysis and derivation, it can be seen that one-dimensional EM can be considered as a special engine operating line under the fixed engine inlet condition. Based on similarity theory, one-dimensional EM with similarity equations, called CEM in this paper, can form a high-dimensional EM. The introduction of similarity equations can not only effectively reduce the requirements of modeling data, but also be more flexible in data selection for modeling. According to the fact that both the steady-state characteristics and the dynamic characteristics are similar when the engine works in a similar state, the CEME model can guarantee global stability by compressing the high-dimensional EM into the one-dimensional EM and using the dynamic characteristics on one-dimensional EM to reflect that on the high-dimensional EM.

Throughout this paper, a series of experiments are carried out to verify the proposed CEME model. The results indicate that the CEME model has a superior precision and calculation stability in capturing dynamic and static behaviors of the aero-engine. Meanwhile, the CEME model is also competent in coping with real-time aero-engine monitoring due to its simple model structure and computer power.

Author Contributions: Conceptualization: L.Z. and J.L.; methodology: L.Z.; validation: Y.M.; supervision: W.Z. and D.Y. All authors have read and agree to the published version of the manuscript.

Funding: This research was funded by the National Natural Science Foundation of China, grant number 51976042, the National Science and Technology Major Project of China, grant number 2017-I-0007-0008 and the National Science and Technology Major Project of China, grant number 2017-V-0005-0055.

Conflicts of Interest: The authors declare no conflict of interest.

References

1. Volponi, A.J. Gas turbine engine health management: Past, present, and future trends. *J. Eng. Gas Turb. Power* **2014**, *136*, 051201. [CrossRef]
2. Holcomb, C.M.; de Callafon, R.A.; Bitmead, R.E. Closed Loop Nonlinear System Identification Applied to Gas Turbine Analytics. In *Turbo. Expo.: Power for Land, Sea, and Air*; American Society of Mechanical Engineers: New York, NY, USA, 2014; Volume 45752, p. V006T06A013.
3. Tahan, M.; Tsoutsanis, E.; Muhammad, M.; Karim, Z. Performance-based health monitoring, diagnostics and prognostics for condition-based maintenance of gas turbines: A review. *Appl. Energy* **2017**, *198*, 122–144. [CrossRef]
4. Yu, D.R.; Sui, Y.F. Expansion Model Based on Equilibrium Manifold for Nonlinear System. *J. Syst. Simul.* **2006**, *18*, 2415–2418.
5. Hu, J.C.; Chang, J.T.; Qin, B.; Wang, L.; Bao, W.; Qin, J. Scramjet Isolator Shock-Train Leading-Edge Position Modeling Based on Equilibrium Manifold. *J. Aerosp. Eng.* **2015**, *28*, 04014064. [CrossRef]
6. Liu, X.; Yuan, Y.T. Nonlinear system modeling and application based on system equilibrium manifold and expansion model. *J. Comput. Nonlin. Dyn.* **2014**, *9*, 021013. [CrossRef]
7. Zhao, H.; Liu, J.F.; Yu, D.R. Approximate nonlinear modeling and feedback linearization control for aeroengines. *ASME J. Eng. Gas. Turbines Power* **2011**, *133*, 111601. [CrossRef]
8. Yan, S.; Jun, Z. A Safety Protection Control Method for Aero-Engines Based on the Switched Equilibrium Manifold Expansion Model. In Proceedings of the 37th IEEE Chinese Control Conference, Wuhan, China, 25–27 July 2018; pp. 2005–2010.
9. He, X.C.; Xiao, L.F. Robust Fault Identification of Turbofan Engines Sensors Based on Fractional-Order Integral Sliding Mode Observer. *Int. J. Turbo Jet Eng.* **2019**. ahead of print. [CrossRef]
10. Yu, D.R.; Zhao, H.; Xu, Z.Q.; Sui, Y.; Liu, J. An approximate nonlinear model for aero-engine control. *P. I. Mech. Eng. G. J. Aer.* **2011**, *255*, 1366–1381.
11. Sui, Y.F.; Yu, D.R. Identification of Expansion Model Based on Equilibrium Manifold of Turbojet Engine. *Acta Aeronaut. Astronaut. Sin. Ser. A B* **2007**, *28*, 531–534.
12. Chen, C.; Zhao, J. Switching Control of Acceleration and Safety Protection for Turbo Fan Aero-Engines Based on Equilibrium Manifold Expansion Model. *Asian J. Control* **2018**, *20*, 1–12. [CrossRef]
13. Shi, Y.; Zhao, J.; Liu, Y.Y. Switching Control for Aero-Engines Based on Switched Equilibrium Manifold Expansion Model. *IEEE Trans. Ind. Electron.* **2017**, *64*, 3156–3165. [CrossRef]
14. Alexander, J.C.; Yorke, J.A. The implicit function theorem and the global methods of cohomology. *J. Funct. Anal.* **1976**, *21*, 330–339. [CrossRef]
15. Stilwell, D.J.; Rugh, W.J. Interpolation of observer state feedback controllers for gain scheduling. *IEEE Trans. Automat. Contr.* **1999**, *44*, 1225–1229. [CrossRef]
16. Giampaolo, T. *Gas Turbine Handbook: Principles and Practice*, 4th ed.; Fairmont Press: New York, NY, USA, 2009; pp. 178–181.
17. Saravanamuttoo, H.H.; Cohen, G.H.; Straznicky, P.V. *Gas Turbine Theory*, 6th ed.; Pearson Education: London, UK, 2001; pp. 178–181.
18. Boyce, M.P. *Gas Turbine Engineering Handbook*, 4th ed.; Elsevier: Oxford, UK, 2012; pp. 11–14.
19. Kang, D.W.; Kim, T.S. Model-based performance diagnostics of heavy-duty gas turbines using compressor map adaptation. *Appl. Energ.* **2018**, *212*, 1345–1359. [CrossRef]